www.cadanda.com
Computer-Aided Design AND APPLICATIONS

NURBS-based Isogeometric Analysis for Small Deformation of Viscoplastic and Creep Problems

Ran Zhang[1,a], Gang Zhao[2,a,b], Wei Wang[3,a], Xiaoxiao Du[4,a], Mayi Guo[5,a]

[a]School of Mechanical Engineering and Automation, Beihang University, Beijing, PR China,
[b]Beijing Engineering Technological Research Center of High-Efficient & Green CNC Machining Process, Beijing, PR China,
[1]Beihang University, feliciamail@buaa.edu.cn
[2]Beihang University, zhaog@buaa.edu.cn
[3]Beihang University, jrrt@buaa.edu.cn
[4]Beihang University, duxiaoxiao@buaa.edu.cn
[5]Beihang University, windowsgmy@126.com

Corresponding author: Wei Wang, jrrt@buaa.edu.cn

Abstract. This paper focuses on the application of NURBS-based isogeometric analysis to viscoplastic and creep problems, in the context of two dimensional small deformation. Viscoplastic materials combining with von Mises yield function and Perzyna's flow rule are employed. The stress expression, stress-strain relationship matrix, isogeometric discrete formulations and other important formulas of viscoplastic and creep problems are derived and listed in detail. Several numerical examples are investigated to verify the proposed method through comparing the results with that from commercial software ABAQUS as well as existing literatures.

Keywords: isogeometric analysis, viscoplastic materials, creep deformation, nonlinear
DOI: https://doi.org/10.14733/cadaps.2021.831-848

1 INTRODUCTION

Finite element analysis (FEA) has been used as a main numerical method to deal with engineering problems [49], such as linear elasticity, transient problems, non-linear problems, contact and impact, applications in fluid dynamics and so on, for many years. Geometrical models are usually discretized into mesh models for FEA, which not only introduces approximation error in the discretization process but also loses certain geometrical information. The gap between CAD and CAE is expected to be bridged by using isogeometric analysis (IGA), proposed by Hughes et al. [11, 23], where the same spline functions are used for both the geometry description in CAD and the analysis model in CAE. In addition, IGA possesses great advantages such as avoiding tedious

meshing processes, realizing adaptive mesh refinement and obtaining more accurate results. And NURBS-based isogeometric analysis has been successfully applied to various engineering practical problems such as structrual shape optimization [45, 40], free vibration [41, 27], plate and shell element [7, 44], fluid-structure interaction analysis [6, 5], even the simulation of non-conforming multi-patch [14, 47, 15] and so on. As for the applications in materials with different constitutive relations, extensive studies on elastic deformation and elastoplastic deformation have been developed. Lorenzis et al. [13] proposed large deformation frictional contact formulation between two 2D elastic bodies. Kiendl et al. [25] explored the large deformation problems of compressible and incompressible hyperelastic thin shells. Nguyen et al. [33] exploited NURBS-based isogeometric approach in solving elastoplastic problems. Benson et al. [8] and Ambati et al. [3] explored elastoplastic deformation of Reissner-Mindlin shell and Kirchhoff-Love shell respectively.

Elastoplastic deformation commonly referred to as plastic deformation, is characterised by irreversiblity and time independence. Permanent deformation will occur in elastoplastic materials once the yield stress point is passed. Note that some materials in life or engineering applications will present a certain degree of time dependency [32, 34]. For example, metal materials under higher temperatures, usually exhibit the phenomena of viscoplasticity and creep simultaneously. The former is a common time dependent plastic deformation and the latter performs the strain-time relationship. The main point of this paper is to derive NURBS-based formulations of viscoplasticity in the small strain range and the calculation of creep deformation can be regarded as a special case of viscoplasticity. Most of the time-dependent models developed so far were applications and extensions of the theory presented by Perzyna [35, 36]. This thoery is so-called overstress model in which the stress is allowed to be outside of the yield surface. Simo and Hughes presented an exhaustive derivation and employed the return mapping algorithms in the strain hardening case [42]. Owen explored the calculation process of finite element analysis for viscoplastic problems [34] and some other researchers [20, 46, 21, 18, 4] have given the summary and application of the relevant FEA formulas. While considering the lack of time-dependent plastic formulas based on isogeometric analysis compared to FEA in the existing literatures and the benefits, i.e. precise geometry representation and higher-order element continuity, of IGA in model construction and calculation, it is a significant and interesting topic to investigate the application of isogeometric analysis on viscoplastic and creep problems.

In this paper, NURBS-based isogeometric analysis is adopted to simulate two dimensional small deformation viscoplastic and creep problems. In Sec. 2, the viscoplastic and creep problems are illustrated and a brief review of NURBS is given. Section 3 describes the formulation of the time-dependent problem using von Mises yield function and Perzyna's flow rule for both viscoplastic and creep deformation. The discretization formulation is presented in detail in Sec. 4. Finally, in Sec. 5 some numerical examples are demonstrated and their results are analyzed and discussed. In addition, the isogeometric analysis for the examples in this paper is based on the NLIGA open source library [16].

2 PRELIMINARIES

2.1 Problem Description

Assume that a body as given in Fig. 1 is in static equilibrium under the applied body force $\boldsymbol{f}^b$ and the surface traction, $\hat{\boldsymbol{t}}^{(\boldsymbol{n})}$, where $\hat{\boldsymbol{t}}^{(\boldsymbol{n})} = \boldsymbol{\sigma} \cdot \boldsymbol{n}$ expresses the stress projection on the surface [10].

Let Ω and Γ denote the domain occupied by the body and the corresponding boundary, respectively. The balance of the linear moment can be stated as

$$\iint_{\Omega} \boldsymbol{f}^b d\Omega + \int_{\Gamma} \hat{\boldsymbol{t}}^{(\boldsymbol{n})} d\Gamma = 0 \tag{1}$$

Considering the expression of $\hat{\boldsymbol{t}}^{(\boldsymbol{n})}$ and the definition of divergence, the second term in the above equation can

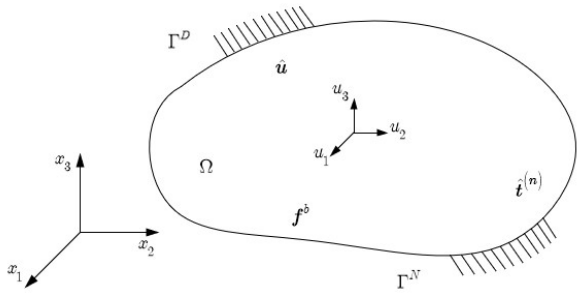

Figure 1: A body in static equilibrium under the applied body force and the surface traction

be converted into the integral over the domain and the above equation can be rewritten as

$$\iint_{\Omega} \boldsymbol{f}^b d\Omega = -\int_{\Gamma} \boldsymbol{\sigma} \cdot \boldsymbol{n} d\Gamma = -\iint_{\Omega} \nabla \cdot \boldsymbol{\sigma} d\Omega \tag{2}$$

and then we obtain

$$\iint_{\Omega} \left(\nabla \cdot \boldsymbol{\sigma} + \boldsymbol{f}^b \right) d\Omega = 0 \tag{3}$$

Assume that the whole boundary Γ can be decomposed into, Γ^D, called Dirichlet boundary condition, and Γ^N, called Neumann boundary condition, which satisfies $\Gamma = \Gamma^D + \Gamma^N$ and $\Gamma^D \cap \Gamma^N = \varnothing$. Considering a body with viscoplastic deformation, the displacement of the structure is prescribed with $\hat{\boldsymbol{u}}$ (or fixed with $\hat{\boldsymbol{u}} = \boldsymbol{0}$) on the boundary Γ^D. In addition, the surface traction is applied on the boundary Γ^N and the body force is distributed in the domain Ω. The purpose of the problem is to find a displacement $\boldsymbol{u}$ that satisfies

$$\begin{aligned} \nabla \cdot \boldsymbol{\sigma} + \boldsymbol{f}^b = \boldsymbol{0} \quad &, \quad x \in \Omega \\ \boldsymbol{u} = \hat{\boldsymbol{u}} \quad &, \quad x \in \Gamma^D \\ \boldsymbol{\sigma} \cdot \boldsymbol{n} = \hat{\boldsymbol{t}}^{(\boldsymbol{n})} \quad &, \quad x \in \Gamma^N \end{aligned} \tag{4}$$

To describe the mathematical model of the viscoplastic problems graphically, we compare the mechanical response of the simple one-dimensional models for time-independent and time-dependent problems, respectively, which are described in detail in reference [42] and now illustrated in Fig. 2.

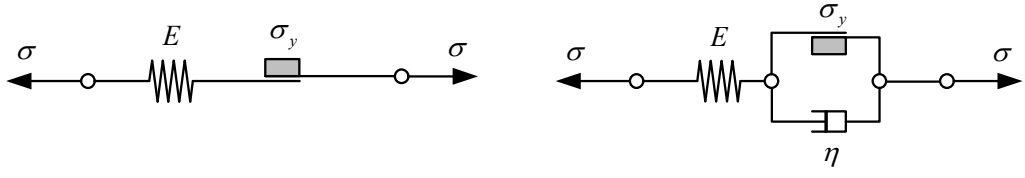

(a) Time-independent problem (b) Time-dependent problem

Figure 2: One-dimensional plastic models

Let σ be the applied stress on the devices and ε is the total strain in the devices. Both the devices in 2a and 2b initially possess unit length and consist of a spring with elastic constant E and a Coulomb friction

element with constant $\sigma_y > 0$. The only difference is that a dashpot, with constant η which is the viscosity parameter symbolized time dependency, is in parallel with the frictional device as shown in Fig. 2b.

With viscoplastic materials assumption [34] here, the devices' total strain, ε, can be separated into elastic, ε^e, and viscoplastic, ε^{vp}, components

$$\varepsilon = \varepsilon^e + \varepsilon^{vp} \tag{5}$$

where ε^e is the strain in the spring, so the stress can be expressed as

$$\sigma = E\varepsilon^e = E\left(\varepsilon - \varepsilon^{vp}\right) \tag{6}$$

For two dimensional case discussed in this paper, equation (6) can be written as

$$\boldsymbol{\sigma} = \boldsymbol{D}\boldsymbol{\varepsilon}^e = \boldsymbol{D}\left(\boldsymbol{\varepsilon} - \boldsymbol{\varepsilon}^{vp}\right) \tag{7}$$

in which $\boldsymbol{D}$ is the elasticity matrix and can be written in plane stress element and plane strain element [26] as

$$\boldsymbol{D} = \frac{E}{1-v^2}\begin{bmatrix} 1 & v & 0 \\ v & 1 & 0 \\ 0 & 0 & \frac{1}{2}(1-v) \end{bmatrix} \text{ or } \boldsymbol{D} = \frac{E}{(1+v)(1-2v)}\begin{bmatrix} 1-v & v & 0 \\ v & 1-v & 0 \\ 0 & 0 & \frac{1}{2}-v \end{bmatrix} \tag{8}$$

where E is the Young's modulus and v is the Poisson's ratio.

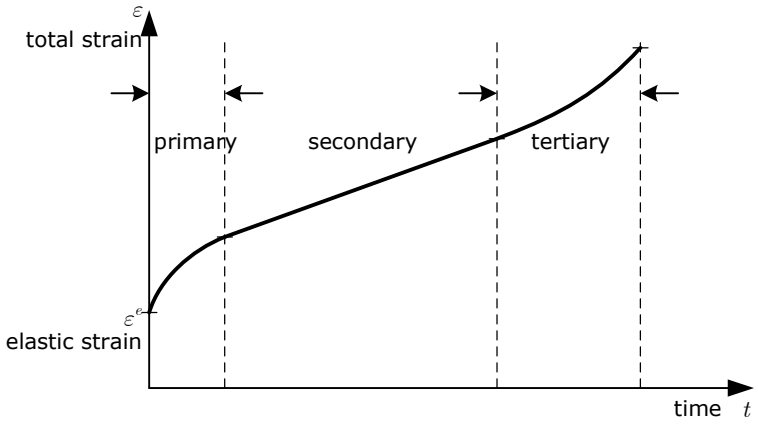

Figure 3: Period of creep

Creep is a slow continuous time-dependent deformation that can be depicted through observing the change in strain over time by applying the load for a long period of time under constant stress and constant room temperature [31]. In general, it can be described, by analyzing the results of creep test on specimens, in terms of three different stages [12] illustrated in Fig. 3. The creep strain rate decreases with increasing time in the initial stage, or primary creep, to a minimum and tends to be a constant which is the beginning of the secondary creep. So the second stage is usually known as the steady-state creep. In tertiary creep, the strain rate increases with time and eventually leads to fracture of the specimen, which is not discussed here [9]. In this paper, the primary and secondary creep stage problems in two-dimensional analysis are in consideration. The related formulas in creep deformation obtained a similar expression by replacing the superscript vp in viscoplastic formulations with c.

2.2 NURBS

The rational representation in Non-uniform Rational B-splines (NURBS) is associated with projective geometry. Except for the coordinates in the physical space, the additional dimension coordinate is called weight, denoted by ω. A NURBS surface can be represented by

$$\boldsymbol{S}(\xi,\eta)=\frac{\sum_{i=0}^{n}\sum_{j=0}^{m}N_{i,p}(\xi)N_{j,q}(\eta)\omega_{ij}\boldsymbol{P}_{ij}}{\sum_{i=0}^{n}\sum_{j=0}^{m}N_{i,p}(\xi)N_{j,q}(\eta)\omega_{ij}} \tag{9}$$

which is also written as

$$\boldsymbol{S}(\xi,\eta)=\sum_{i=0}^{n}\sum_{j=0}^{m}R_{i,j}^{p,q}(\xi,\eta)\boldsymbol{P}_{ij} \tag{10}$$

$$R_{i,j}^{p,q}(\xi,\eta)=\frac{N_{i,p}(\xi)N_{j,q}(\eta)\omega_{ij}}{\sum_{k=0}^{n}\sum_{l=0}^{m}N_{k,p}(\xi)N_{l,q}(\eta)\omega_{kl}} \tag{11}$$

where $\boldsymbol{P}_{ij}$ and ω_{ij} represent the coordinates of control points and the corresponding weights respectively. n and m are the number of control points in the two directions subtracting 1 respectively. $N_{i,p}$ is the p-th B-splines basis function which can be defined with an open knot vector $\Xi=\{\xi_0,\xi_1,\ldots,\xi_{n+p+1}\}$ by Cox-deBoor recursive formulas as

$$\begin{aligned}N_{i,0}(\xi)&=\begin{cases}1 & \xi_i\le\xi<\xi_{i+1}\\ 0 & \textit{otherwise}\end{cases}\\ N_{i,p}(\xi)&=\frac{\xi-\xi_i}{\xi_{i+p}-\xi_i}N_{i,p-1}(\xi)+\frac{\xi_{i+p+1}-\xi}{\xi_{i+p+1}-\xi_{i+1}}N_{i+1,p-1}(\xi)\quad p\ge1\end{cases} \tag{12}$$

For more details about NURBS we recommend the literature [37].

3 FORMULATION

3.1 Basic Formulations of Time-dependent Deformation

According to the relevant literature [35, 36, 39, 29, 48, 43, 17, 2, 30, 20, 46, 21, 18, 4] in which previous researches have given formulas for solving viscoplastic problems based on finite element analysis, we derived and sorted out the following viscoplastic formulas which are applied to isogeometric analysis in our paper.

Considering the time-dependency property of the viscoplastic materials, it is now necessary to determine a flow rule defining the viscoplastic strain rate and to obtain the stress by Eq. (7) further. The stress rate can be expressed as

$$\dot{\boldsymbol{\sigma}}=\boldsymbol{D}\dot{\boldsymbol{\varepsilon}}^{e}=\boldsymbol{D}\left(\dot{\boldsymbol{\varepsilon}}-\dot{\boldsymbol{\varepsilon}}^{vp}\right) \tag{13}$$

An explicit form is one, simplified from the viscoplastic theory proposed by Perzyna [35], in which the viscoplastic strain rate depends only on the current stresses, so that

$$\dot{\boldsymbol{\varepsilon}}^{vp}=\frac{1}{\eta}\langle f(\boldsymbol{\sigma})\rangle\frac{\partial f(\boldsymbol{\sigma})}{\partial\boldsymbol{\sigma}} \tag{14}$$

where η is the viscosity parameter as shown in Fig. 2b and the notation $\langle\ \rangle$ implies the ramp function $\langle x\rangle=\frac{x+|x|}{2}$. In addition, $f(\boldsymbol{\sigma})=\|\boldsymbol{s}\|-\sqrt{\frac{2}{3}}\sigma_y$ is the yield function in von Mises type wherein $\boldsymbol{s}$ is the deviatoric stress and σ_y is the initial yield stress of the plastic material.

It is obvious that "time" is one of the most important parameters in the time-dependent problem and we divided the total time T into finite time intervals denoted by $t=\left[\ t_0,\quad t_1,\quad\cdots,\quad t_{\text{end}}\ \right]$, where $t_0=0$ is

the initial time and $t_{\text{end}} = T$ is the final time. In addition, $t_n (n = 0, 1, \cdots, end)$ is called time t_n and for two adjacent times t_{n-1} and t_n there exists $t_n = t_{n-1} + \Delta t_n$. The time interval Δt_n can be calculated in von Mises material as

$$\Delta t_n \leq k \Delta t_{n-1} \quad \text{and} \quad \Delta t_n \leq \frac{4(1+v)\sigma_y}{3E/\eta} \tag{15}$$

wherein $k = 1.5$ is suitable from experiences [34]. With the implicit time integration scheme, the viscoplastic strain increment $\Delta \boldsymbol{\varepsilon}_n^{vp}$ generated in time interval $\Delta t_n = t_n - t_{n-1}$ can be calculated as

$$\Delta \boldsymbol{\varepsilon}_n^{vp} = \Delta t_n \left[(1-\theta) \dot{\boldsymbol{\varepsilon}}_{n-1}^{vp} + \theta \dot{\boldsymbol{\varepsilon}}_n^{vp} \right] \tag{16}$$

in which $\theta = \frac{1}{2}$ represents the so-called 'implicit trapezoidal' time integration scheme since the viscoplastic strain increment is generated by conditions at time t_{n-1} and t_n. If $\theta = 0$, it is called fully explicit scheme and $\theta = 1$ corresponds to the so-called fully implicit scheme. The strain increment for these two schemes can be determined by the strain rate at the start and the end of the time interval, respectively. The viscoplastic strain rate $\dot{\boldsymbol{\varepsilon}}_{n-1}^{vp}$ at time t_n is computed from Eq. (14) with $\boldsymbol{\sigma} = \boldsymbol{\sigma}_{n-1}$. While $\dot{\boldsymbol{\varepsilon}}_n^{vp}$ is unknown at time t_n and can be obtained according to Taylor's formula as

$$\dot{\boldsymbol{\varepsilon}}_n^{vp} = \dot{\boldsymbol{\varepsilon}}_{n-1}^{vp} + \left(\frac{\partial \dot{\boldsymbol{\varepsilon}}^{vp}}{\partial \boldsymbol{\sigma}} \right)_{n-1} \Delta \boldsymbol{\sigma}_n = \dot{\boldsymbol{\varepsilon}}_{n-1}^{vp} + \boldsymbol{H}_{n-1} \Delta \boldsymbol{\sigma}_n \tag{17}$$

where $\boldsymbol{H}_{n-1} = \left(\frac{\partial \dot{\boldsymbol{\varepsilon}}^{vp}}{\partial \boldsymbol{\sigma}} \right)_{n-1}$ is the derivative of the viscoplastic strain rate with respect to the stress at time t_{n-1} and will be presented later. Thus the expression of viscoplastic strain increment in Eq. (16) can be rewritten as

$$\begin{aligned} \Delta \boldsymbol{\varepsilon}_n^{vp} &= \Delta t_n \left[(1-\theta) \dot{\boldsymbol{\varepsilon}}_{n-1}^{vp} + \theta \left(\dot{\boldsymbol{\varepsilon}}_{n-1}^{vp} + \boldsymbol{H}_{n-1} \Delta \boldsymbol{\sigma}_n \right) \right] \\ &= \Delta t_n \dot{\boldsymbol{\varepsilon}}_{n-1}^{vp} + \theta \Delta t_n \boldsymbol{H}_{n-1} \Delta \boldsymbol{\sigma}_n = \Delta t_n \dot{\boldsymbol{\varepsilon}}_{n-1}^{vp} + \boldsymbol{C}_{n-1} \Delta \boldsymbol{\sigma}_n \end{aligned} \tag{18}$$

in which $\boldsymbol{C}_{n-1} = \theta \Delta t_n \boldsymbol{H}_{n-1}$ if $\theta \neq 0$ and $\Delta \boldsymbol{\sigma}_n$ is the stress increment at the time interval Δt_n which can be calculated analogously with Eq. (7) as

$$\Delta \boldsymbol{\sigma}_n = \boldsymbol{D} \left(\Delta \boldsymbol{\varepsilon}_n - \Delta \boldsymbol{\varepsilon}_n^{vp} \right) \tag{19}$$

Substituting Eq. (18) and $\Delta \boldsymbol{\varepsilon}_n = \varepsilon \left(\Delta \boldsymbol{u}_n \right)$, which will be discussed in the next section, into Eq. (19), the expression of stress increment with respect to the unknown displacement increment can be rewritten as

$$\Delta \boldsymbol{\sigma}_n = \left(\boldsymbol{D}^{-1} + \boldsymbol{C}_{n-1} \right)^{-1} \left(\varepsilon \left(\Delta \boldsymbol{u}_n \right) - \Delta t_n \dot{\boldsymbol{\varepsilon}}_{n-1}^{vp} \right) = \boldsymbol{D}_n \left(\varepsilon \left(\Delta \boldsymbol{u}_n \right) - \Delta t_n \dot{\boldsymbol{\varepsilon}}_{n-1}^{vp} \right) \tag{20}$$

where $\boldsymbol{D}_n = \left(\boldsymbol{D}^{-1} + \boldsymbol{C}_{n-1} \right)^{-1}$ is the matrix of stress-strain relationship at time t_n.

Creep strain appears even in the elastic stage for creep problems. So the creep strain rate can be expressed by assigning the initial yield stress to zero [22, 28] in Eq. (14). In secondary creep the strain rate is a constant and can be written without time as

$$\dot{\boldsymbol{\varepsilon}}^c = \frac{1}{\eta} \| \boldsymbol{s} \| \frac{\partial \| \boldsymbol{s} \|}{\partial \boldsymbol{\sigma}} \tag{21}$$

In primary creep problem, the creep strain rate is regarded as the function of time and equation (21) can be rewritten as

$$\dot{\boldsymbol{\varepsilon}}^c = \frac{1}{\eta} \| \boldsymbol{s} \| \frac{\partial \| \boldsymbol{s} \|}{\partial \boldsymbol{\sigma}} \cdot t^m \tag{22}$$

where m is a given constant number ranges $(-1, 0]$ and if $m = 0$ this problem becomes the secondary creep problem. The rest calculation of the primary and secondary creep problem is similar with viscoplastic problem.

3.2 The Weak Form of Governing Equations

With the strong form of the aforementioned governing equations (1), (2), (3), the weak form of governing equations can be obtained. Then the potential energy $\Pi(\boldsymbol{u})$ of the viscoplastic structure can be expressed as the difference between the strain energy $W^{int}(\boldsymbol{u})$ and the work $W^{ext}(\boldsymbol{u})$ done by the applied loads, written as

$$\Pi(\boldsymbol{u}) = W^{int}(\boldsymbol{u}) - W^{ext}(\boldsymbol{u}) \tag{23}$$

where

$$W^{int}(\boldsymbol{u}) = \frac{1}{2}\iint_{\Omega} \boldsymbol{\sigma} : \boldsymbol{\varepsilon}^{e} d\Omega = \frac{1}{2}\iint_{\Omega} \boldsymbol{\sigma} : (\boldsymbol{\varepsilon} - \boldsymbol{\varepsilon}^{vp})\, d\Omega \tag{24}$$

$$W^{ext}(\boldsymbol{u}) = \iint_{\Omega} \boldsymbol{u} \cdot \boldsymbol{f}^{b} d\Omega - \int_{\Gamma} \boldsymbol{u} \cdot \hat{\boldsymbol{t}}^{(\boldsymbol{n})} d\Gamma \tag{25}$$

The unknown variable of the total potential energy is the nodal displacement of the structure. According to the principle of minimum potential energy and the variational principle, the minimum potential can be obtained when the first variation of the total potential energy equal to zero, as

$$\delta\Pi(\boldsymbol{u}, \delta\boldsymbol{u}) = \delta W^{int}(\boldsymbol{u}, \delta\boldsymbol{u}) - \delta W^{ext}(\delta\boldsymbol{u}) \tag{26}$$

which is called the variational equation of the structural problem under consideration [38]. The first term is obtained from the definition of $W^{int}(\boldsymbol{u})$ and stress-strain relation as

$$\delta W^{int}(\boldsymbol{u}, \delta\boldsymbol{u}) = \iint_{\Omega} \boldsymbol{\varepsilon}(\delta\boldsymbol{u}) : \boldsymbol{D} : (\boldsymbol{\varepsilon} - \boldsymbol{\varepsilon}^{vp})\, d\Omega = a(\boldsymbol{u}, \delta\boldsymbol{u}) \tag{27}$$

where $a(\boldsymbol{u}, \delta\boldsymbol{u})$ is called the energy form. The second term is the variation of the work done by the applied load and can be written as

$$\delta W^{ext}(\delta\boldsymbol{u}) = \iint_{\Omega} \delta\boldsymbol{u} \cdot \boldsymbol{f}^{b} d\Omega - \int_{\Gamma} \delta\boldsymbol{u} \cdot \hat{\boldsymbol{t}}^{(\boldsymbol{n})} d\Gamma = l(\delta\boldsymbol{u}) \tag{28}$$

where $l(\delta\boldsymbol{u})$ is called the load form. Only conservative loads are considered such that $l(\delta\boldsymbol{u})$ is independent of displacement $\boldsymbol{u}$. Thus, the equations of equilibrium, Eq. (26), can be written at any instant of time t_n as

$$\int_{\Omega} \boldsymbol{B}_n^{T} \boldsymbol{\sigma}_n d\Omega = \boldsymbol{f}_n \tag{29}$$

in which $\boldsymbol{B}_n$ is the strain-displacement matrix which will not vary during the solution of small deformation [11] and it can be equivalent to $\boldsymbol{B}$ omitting the subscript and introducing in the subsequent chapter. $\boldsymbol{f}_n$ is equivalent nodal loads due to the applied surface traction $\hat{\boldsymbol{t}}^{(\boldsymbol{n})}$ and the body force $\boldsymbol{f}^{b}$. Linearizing the weak form of governing equations, the incremental form during the time interval Δt_n can be written as

$$\int_{\Omega} \boldsymbol{B}_n^{T} \Delta\boldsymbol{\sigma}_n d\Omega = \Delta\boldsymbol{f}_n \tag{30}$$

and substituting for $\Delta\boldsymbol{\sigma}_n$ from Eq. (20) the above equation becomes

$$\int_{\Omega} \boldsymbol{B}^{T} \boldsymbol{D}_n \boldsymbol{B} \Delta\boldsymbol{u}_n d\Omega = \int_{\Omega} \boldsymbol{B}^{T} \boldsymbol{D}_n \Delta t_n \dot{\boldsymbol{\varepsilon}}_{n-1}^{vp} d\Omega + \Delta\boldsymbol{f}_n \tag{31}$$

Considering the nonlinearity of the viscoplastic problem and the viscoplastic strain rate was approximately calculated at time t_n by Taylor's formula, the residual is inevitable and can be given by

$$\boldsymbol{R} = l(\delta \boldsymbol{u}) - a(\boldsymbol{u}, \delta \boldsymbol{u}) \Rightarrow \boldsymbol{R}_n = \int_\Omega \boldsymbol{B}_n^T \boldsymbol{\sigma}_n d\Omega - \boldsymbol{f}_n \tag{32}$$

The complexity caused by the Newton-Raphson iteration can be avoided effectively by adding the residual to the incremental equilibrium equation at the next time interval Δt_{n+1} as

$$\int_\Omega \boldsymbol{B}^T \boldsymbol{D}_{n+1} \boldsymbol{B} \Delta \boldsymbol{u}_{n+1} d\Omega = \int_\Omega \boldsymbol{B}^T \boldsymbol{D}_{n+1} \Delta t_{n+1} \dot{\boldsymbol{\varepsilon}}_n^{vp} d\Omega + \Delta \boldsymbol{f}_{n+1} + \boldsymbol{R}_n \tag{33}$$

The discretized isogeometric equations derived for small strain viscoplastic problem can be written as

$$\boldsymbol{K}_{n+1} \Delta \boldsymbol{u}_{n+1} = \boldsymbol{F}_{n+1} \tag{34}$$

Then the displacement increment $\boldsymbol{u}_{n+1}$ at time interval Δt_{n+1} can be obtained by solving the above equations and the total displacement can be obtained by adding the displacement increment at each time interval. The representation of the strain-displacement matrix $\boldsymbol{B}$, the stiffness matrix $\boldsymbol{K}_{n+1}$ and the residual force $\boldsymbol{F}_{n+1}$ will be discussed in the next section.

4 ISOGEOMETRIC DISCRETIZATION

For the numerical studies based on isogeometric analysis in this paper, the displacement, $\boldsymbol{u}(\xi, \eta)$, of an arbitrary point on a NURBS surface can be interpolated by the displacement of related control points and its corresponding basis functions [23, 37] as

$$\boldsymbol{u}(\xi, \eta) = \sum_{i=0}^{n} \sum_{j=0}^{m} R_{i,j}^{p,q}(\xi, \eta) \boldsymbol{u}_{ij} \tag{35}$$

Considering the convenience of calculation and storage in program, rearrange the basis functions $R_{i,j}^{p,q}(\eta, \xi) = \left[R_{0,0}^{p,q}(\eta, \xi), R_{0,1}^{p,q}(\eta, \xi), \cdots, R_{0,m}^{p,q}(\eta, \xi), R_{1,0}^{p,q}(\eta, \xi), R_{1,1}^{p,q}(\eta, \xi), \cdots, R_{1,m}^{p,q}(\eta, \xi), \cdots, R_{n,0}^{p,q}(\eta, \xi), \cdots, R_{n,m}^{p,q}(\eta, \xi)\right]$ of the surface into $R_i(\eta, \xi) = [R_0(\eta, \xi), R_1(\eta, \xi), \cdots, R_{ncp}(\eta, \xi)]$ and the above equation (35) can be rewritten as

$$\boldsymbol{u}(\xi, \eta) = \sum_{i=0}^{ncp} R_i(\xi, \eta) \boldsymbol{u}_i \tag{36}$$

where ncp equals the number of control points subtracting 1. The parameter (ξ, η) will be omitted in the following descriptions for simplicity. In two dimensional problems, the matrix expression of the displacement can be written as

$$\boldsymbol{u} = \begin{bmatrix} u \\ v \end{bmatrix} = \boldsymbol{R} \bar{\boldsymbol{u}} \tag{37}$$

with

$$\boldsymbol{R} = \begin{bmatrix} R_0 & 0 & R_1 & 0 & \cdots & R_{ncp} & 0 \\ 0 & R_0 & 0 & R_1 & \cdots & 0 & R_{ncp} \end{bmatrix} \tag{38}$$

$$\bar{\boldsymbol{u}} = \begin{bmatrix} u_0 & v_0 & u_1 & v_1 & \cdots & u_{ncp} & v_{ncp} \end{bmatrix}^T \tag{39}$$

where the superscript T denotes the transpose of matrix or vector. According to the strain-displacement relationship, the total strain in small deformation of the plane strain element can be calculated by the partial derivative of the displacements versus coordinates [11] as

$$\boldsymbol{\varepsilon} = \boldsymbol{B}\bar{\boldsymbol{u}} = \begin{bmatrix} \varepsilon_{11} & \varepsilon_{22} & \varepsilon_{12} \end{bmatrix}^T \tag{40}$$

with the strain-displacement matrix

$$\boldsymbol{B} = \begin{bmatrix} \frac{\partial R_0}{\partial x} & 0 & \frac{\partial R_1}{\partial x} & 0 & \cdots & \frac{\partial R_{ncp}}{\partial x} & 0 \\ 0 & \frac{\partial R_0}{\partial y} & 0 & \frac{\partial R_1}{\partial y} & \cdots & 0 & \frac{\partial R_{ncp}}{\partial y} \\ \frac{\partial R_0}{\partial y} & \frac{\partial R_0}{\partial x} & \frac{\partial R_1}{\partial y} & \frac{\partial R_1}{\partial x} & \cdots & \frac{\partial R_{ncp}}{\partial y} & \frac{\partial R_{ncp}}{\partial x} \end{bmatrix} \tag{41}$$

As for the plane stress element, the total strain can be written as

$$\underset{4\times 1}{\boldsymbol{\varepsilon}} = \begin{bmatrix} \varepsilon_{11} & \varepsilon_{22} & \varepsilon_{12} & \vdots & \varepsilon_{33} \end{bmatrix}^T \tag{42}$$

in which the first three terms can be obtained similarly from Eq. (40) and the fourth component can be calculated by $\varepsilon_{33} = -\frac{v}{1-v}(\varepsilon_{11} + \varepsilon_{22})$. The increment of strain $\Delta\boldsymbol{\varepsilon}$ used in the above equations can be obtained by adding an incremental symbol Δ before the strain $\boldsymbol{\varepsilon}$.

The deviatoric stress $\boldsymbol{s}$ in the yield function can be expressed as

$$\boldsymbol{s} = \begin{bmatrix} s_{11} & s_{12} & 0 \\ s_{21} & s_{22} & 0 \\ 0 & 0 & s_{33} \end{bmatrix} = \begin{bmatrix} \frac{2}{3}\sigma_{11} - \frac{1}{3}\sigma_{22} & \sigma_{12} & 0 \\ \sigma_{21} & \frac{2}{3}\sigma_{22} - \frac{1}{3}\sigma_{11} & 0 \\ 0 & 0 & -\frac{1}{3}\sigma_{11} - \frac{1}{3}\sigma_{22} \end{bmatrix} \tag{43}$$

for plane stress element. For plane strain element there exists $\sigma_{33} = v(\sigma_{11} + \sigma_{22})$ and the deviatoric stress can be given by

$$\boldsymbol{s} = \begin{bmatrix} s_{11} & s_{12} & 0 \\ s_{21} & s_{22} & 0 \\ 0 & 0 & s_{33} \end{bmatrix} = \begin{bmatrix} \frac{2}{3}\sigma_{11} - \frac{1}{3}\sigma_{22} - \frac{1}{3}\sigma_{33} & \sigma_{12} & 0 \\ \sigma_{21} & \frac{2}{3}\sigma_{22} - \frac{1}{3}\sigma_{11} - \frac{1}{3}\sigma_{33} & 0 \\ 0 & 0 & \frac{2}{3}\sigma_{33} - \frac{1}{3}\sigma_{11} - \frac{1}{3}\sigma_{22} \end{bmatrix} \tag{44}$$

The von Mises equivalent stress, $\|\boldsymbol{s}\|$, can be calculated as

$$\|\boldsymbol{s}\| = \sqrt{\sigma_{11}^2 + \sigma_{22}^2 - \sigma_{11}\sigma_{22} + 3\sigma_{12}^2} \tag{45}$$

and

$$\|\boldsymbol{s}\| = \sqrt{\sigma_{11}^2 + \sigma_{22}^2 + \sigma_{33}^2 - \sigma_{11}\sigma_{22} - \sigma_{22}\sigma_{33} - \sigma_{33}\sigma_{11} + 3\sigma_{12}^2} \tag{46}$$

for plane stress element and plane strain element, respectively.

The stiffness matrix $\boldsymbol{K}_{n+1}$ at time t_{n+1} is calculated by

$$\boldsymbol{K}_{n+1} = \int_\Omega \boldsymbol{B}^T \boldsymbol{D}_{n+1} \boldsymbol{B} d\Omega = \int_\Omega \boldsymbol{B}^T \left(\boldsymbol{D}^{-1} + \boldsymbol{C}_n\right)^{-1} \boldsymbol{B} d\Omega = \int_\Omega \boldsymbol{B}^T \left(\boldsymbol{D}^{-1} + \theta \Delta t_{n+1} \boldsymbol{H}_n\right)^{-1} \boldsymbol{B} d\Omega \tag{47}$$

in which $\boldsymbol{H}_n = \left(\frac{\partial \dot{\boldsymbol{\varepsilon}}^{vp}}{\partial \boldsymbol{\sigma}}\right)_n$ is related with the variables at time t_n and the matrix $\boldsymbol{H}$ for any given subscript n can be written as

$$\boldsymbol{H} = c_1 \boldsymbol{S}_1 + c_2 \boldsymbol{S}_2 \tag{48}$$

where c_1 and c_2 are scalars with forms

$$c_1 = \frac{3}{2\eta} \times f(\boldsymbol{\sigma}) \times \frac{1}{\|\boldsymbol{s}\|} \text{ and } c_2 = \frac{9}{4\eta} \times \frac{1}{\|\boldsymbol{s}\|^2} \times \left(1 - \frac{f(\boldsymbol{\sigma})}{\|\boldsymbol{s}\|}\right) \tag{49}$$

For the plane stress element

$$\boldsymbol{S}_1 = \begin{bmatrix} \frac{2}{3} & -\frac{1}{3} & 0 \\ -\frac{1}{3} & \frac{2}{3} & 0 \\ 0 & 0 & 2 \end{bmatrix} \text{ and } \boldsymbol{S}_2 = \begin{bmatrix} {s_{11}}^2 & s_{11}s_{22} & 2s_{11}s_{12} \\ s_{11}s_{22} & {s_{22}}^2 & 2s_{22}s_{12} \\ 2s_{11}s_{12} & 2s_{22}s_{12} & 4{s_{12}}^2 \end{bmatrix} \tag{50}$$

and for the plane strain element

$$\boldsymbol{S}_1 = \begin{bmatrix} \frac{2}{3} & -\frac{1}{3} & 0 & -\frac{1}{3} \\ -\frac{1}{3} & \frac{2}{3} & 0 & -\frac{1}{3} \\ 0 & 0 & 2 & 0 \\ -\frac{1}{3} & -\frac{1}{3} & 0 & \frac{2}{3} \end{bmatrix} \text{ and } \boldsymbol{S}_2 = \begin{bmatrix} {s_{11}}^2 & s_{11}s_{22} & 2s_{11}s_{12} & s_{11}s_{33} \\ s_{11}s_{22} & {s_{22}}^2 & 2s_{22}s_{12} & s_{22}s_{33} \\ 2s_{11}s_{12} & 2s_{22}s_{12} & 4{s_{12}}^2 & 2s_{12}s_{33} \\ s_{11}s_{33} & s_{22}s_{33} & 2s_{12}s_{33} & {s_{33}}^2 \end{bmatrix} \tag{51}$$

The fourth row and fourth column in Eq. (51) are not considered in the actual calculation and it can also be written as Eq. (50).

The residual force $\boldsymbol{F}_{n+1}$ is calculated by

$$\boldsymbol{F}_{n+1} = \int_\Omega \boldsymbol{B}^T \boldsymbol{D}_{n+1} \Delta t_{n+1} \dot{\boldsymbol{\varepsilon}}_n^{vp} d\Omega + \Delta \boldsymbol{f}_{n+1} + \boldsymbol{R}_n \tag{52}$$

where $\boldsymbol{D}_{n+1}$ is the same as in Eq. (47).

Based on the above formulas, the essential steps for solving viscoplastic problems by isogeometric analysis can be summarised. Considering the initial state at time t_0 is static elasticity and of course viscoplastic deformation has not occurred and the viscoplastic strain has $\varepsilon_0^{vp} = 0$. Assuming that the variables such as $\bar{\boldsymbol{u}}_n$, $\boldsymbol{\varepsilon}_n$, $\boldsymbol{\sigma}_n$, ε_n^{vp}, $\dot{\boldsymbol{\varepsilon}}_n^{vp}$ and the residual $\boldsymbol{R}_n$ at time t_n are known and the variables at time t_{n+1}, which satisfies $t_{n+1} < t_{end} = T$ simultaneously, can be calculated as follows:

1. Suppose the state is viscoplastic and satisfies the governing equations at time t_{n+1} and the matrices depend on the variables at time t_n can be obtained

$$\boldsymbol{H}_n = \left(\frac{\partial \dot{\boldsymbol{\varepsilon}}^{vp}}{\partial \boldsymbol{\sigma}}\right)_n, \quad \boldsymbol{C}_n = \theta \Delta t_{n+1} \boldsymbol{H}_n, \quad \boldsymbol{D}_{n+1} = \left(\boldsymbol{D}^{-1} + \boldsymbol{C}_n\right)^{-1}, \quad \boldsymbol{K}_{n+1} = \int_\Omega \boldsymbol{B}^T \boldsymbol{D}_{n+1} \boldsymbol{B} d\Omega \tag{53}$$

2. Compute the displacement increment $\Delta \bar{\boldsymbol{u}}_{n+1}$ according to Eqs. (34) and (52) as

$$\Delta \bar{\boldsymbol{u}}_{n+1} = \boldsymbol{K}_{n+1}^{-1} \boldsymbol{F}_{n+1} \tag{54}$$

3. Compute the stress increment $\Delta \boldsymbol{\sigma}_{n+1}$ as

$$\Delta \boldsymbol{\sigma}_{n+1} = \boldsymbol{D}_{n+1} \left(\boldsymbol{B} \Delta \bar{\boldsymbol{u}}_{n+1} - \Delta t_{n+1} \dot{\boldsymbol{\varepsilon}}_n^{vp}\right) \tag{55}$$

4. The total displacement and stress at time t_{n+1} can be obtained as

$$\bar{\boldsymbol{u}}_{n+1} = \bar{\boldsymbol{u}}_n + \Delta \bar{\boldsymbol{u}}_{n+1}, \quad \boldsymbol{\sigma}_{n+1} = \boldsymbol{\sigma}_n + \Delta \boldsymbol{\sigma}_{n+1} \tag{56}$$

5. Compute the viscoplastic strain rate $\dot{\boldsymbol{\varepsilon}}^{vp}_{n+1}$ as

$$\dot{\boldsymbol{\varepsilon}}^{vp}_{n+1} = \dot{\boldsymbol{\varepsilon}}^{vp}_{n} + \boldsymbol{H}_n \Delta\boldsymbol{\sigma}_{n+1} \tag{57}$$

6. The residual needs to be considered now and it can be calculated like Eq. (32) as

$$\boldsymbol{R}_{n+1} = \int_{\Omega} \boldsymbol{B}^T_{n+1}\boldsymbol{\sigma}_{n+1} d\Omega - \boldsymbol{f}_{n+1} = \int_{\Omega} \boldsymbol{B}^T\boldsymbol{\sigma}_{n+1} d\Omega - \boldsymbol{f}_{n+1} \tag{58}$$

Then the residual force for the next time intervial can be obtained by simple addition in Eq. (52)

7. Determine the next time interval Δt_{n+2} by the following inequality

$$\Delta t_{n+2} \leq k\Delta t_{n+1} \quad \text{and} \quad \Delta t_{n+2} \leq \frac{4(1+v)\sigma_y}{3E/\eta} \tag{59}$$

or if $t_{n+2} = t_{n+1} + \Delta t_{n+2} > t_{end} = T$, Δt_{n+2} can be determined as

$$\Delta t_{n+2} = T - t_{n+1} \tag{60}$$

8. Check whether the current state is still viscoplastic, in other words, whether the viscoplastic strain rate $\dot{\boldsymbol{\varepsilon}}^{vp}_{n+1}$ is nonzero at a certain Gauss integral point.

8.a) If so return to step 1 and repeat the above steps.

8.b) If $\dot{\boldsymbol{\varepsilon}}^{vp}_{n+1}$ at all Gauss integral points is extremely close to zero, a steady state is considered to be reached and it is time to end the algorithm. Then the final state is the steady state at time t_{n+1}.

5 NUMERICAL EXAMPLES

5.1 Viscoplastic Deformation of A Plate with A Hole

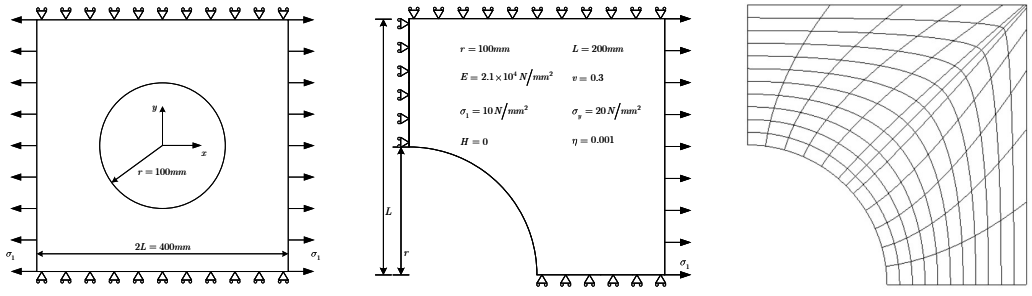

(a) Problem description (b) Symmetric modeling (c) Mesh of the model

Figure 4: Problem description and simplified model for the plate with a hole. (a) the plate with a hole, (b) the material and boundary condition of the simplified model, (c) the mesh of the model.

A plane strain plate with a hole, see Fig. 4a, has been simulated because it is a problem previously discussed in the literatures [19, 2]. The geometry is a square plate with a hole in its center. Due to the symmetry of the problem it is equivalent to consider only a quarter of the sample and the simplified conditions are imposed as illustrated in Fig. 4b. The solutions of the viscoplastic problem are developed on a NURBS model with

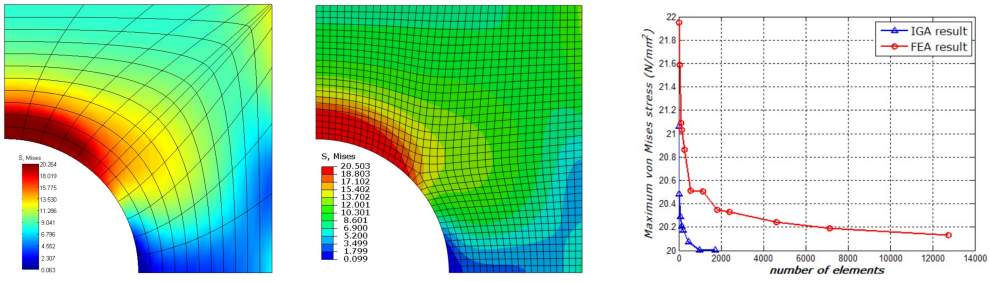

(a) IGA result (b) ABAQUS result (c) Comparison

Figure 5: von Mises stress (units: N/mm^2) result in comparison. (a) the result from IGA program, (b) the result from ABAQUS, (c) comparison of maximum von Mises stress-elements curves between IGA and FEA.

12×11 elements and 3×3 degrees as given in Fig. 4c. Meanwhile, this problem was solved in ABAQUS with 3541 nodes and 1130 CPE8R elements where CPE8R denotes an 8-node biquadratic plane strain quadrilateral elements with reduced integration [1].

Figure 5 presents the results of the von Mises equivalent stress denoted by S,Mises based on the IGA model and FEA model, where the distributions of S,Mises obtained from isogeometric analysis and ABAQUS by using finite element method are given in Figs. 5a and 5b, respectively. As expected, it can be seen that the distributions of von Mises stress calculated from IGA and ABAQUS agree very well. As shown in Fig. 5c, the maximum von Mises stress under viscoplastic deformation of a plate with a hole are obtained on biquadratic plane strain quadrilateral elements by using IGA and ABAQUS, respectively. The horizontal axis denotes the number of elements and the vertical axis denotes the maximum value of von Mises stress on the plate with a hole. It can be found that the maximum von Mises stress-elements curves obtained by using two different methods converge to a very close result. In other words, at the same biquadratic elements the maximum von Mises stress are asymptotic as the number of elements increases. Note that the NURBS model in isogeometric analysis with fewer number of elements can converge to the stable value faster than FEA.

5.2 Viscoplastic Deformation of A Thick Cylinder

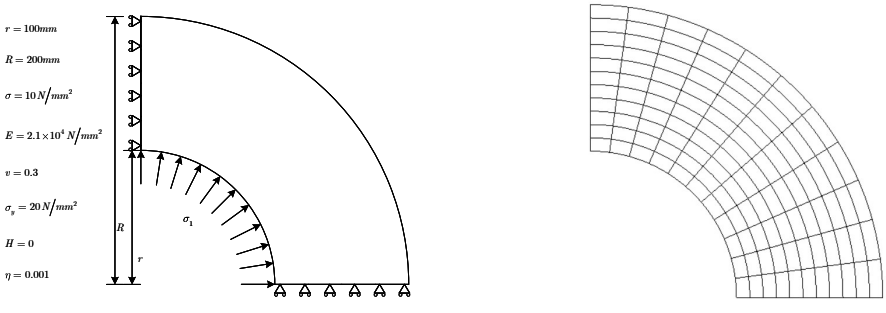

(a) Problem description (b) Mesh of the model

Figure 6: Problem description and simplified model for the thick cylinder. (a) the material and boundary condition of the underside of the simplified model, (b) the mesh of the model.

Similar to the simplification principle of the previous example, the underside of a quarter of the thick

cylinder subjected to a constant internal pressure as given in Fig. 6a was previously studied in [24] by using the finite element method and is also investigated here by employing the isogeometric method. Figure 6b shows the NURBS model with 11×11 elements and degrees 3×3. As for the solution in ABAQUS, 2295 nodes and 940 CPE8R elements are used and von Mises yield criterion is considered.

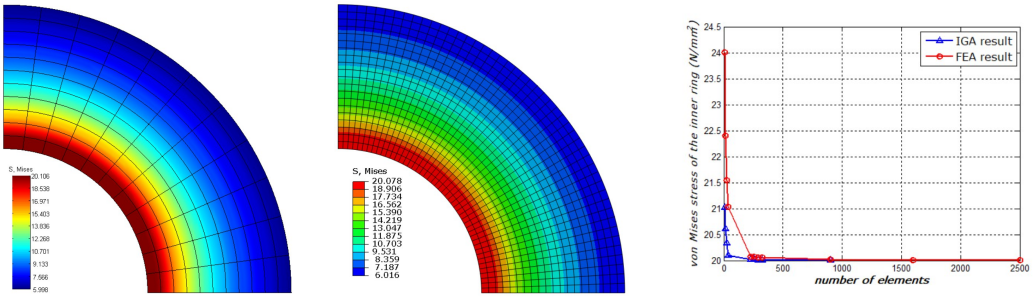

(a) IGA result (b) ABAQUS result (c) Comparison

Figure 7: von Mises stress (units: N/mm^2) result in comparison. (a) the result from IGA program, (b) the result from ABAQUS, (c) comparison of von Mises stress-elements curves between IGA and FEA.

Figure 7a shows the contour of the von Mises stress based on the IGA method. For the comparison, the problem is also simulated in ABAQUS [1] and the stress result is provided in Fig. 7b. We can see that the distributions of von Mises stress in the quarter cylinder calculated by the two methods are in good agreement. The curves in Fig. 7c show the relationship between the von Mises stress of the inner ring of the cylinder and the number of elements at the same degree, i.e. the number of biquadratic elements. We can see that the stress tends to be the same as the number of elements increases and the result in isogeometric analysis reaches the stable value faster.

The above two examples in Sec. 5.1 and Sec. 5.2 show that it is feasible and efficient to calculate the two dimensional small deformation of viscoplastic problem with isogeometric analysis method.

5.3 Creep Deformation of A Square Plate

As for the example of creep, we are going to study the creep deformation problems of a square plate with length 100×100 under various combinations of boundary conditions, element types and creep stages. The results of magnitude displacement are calculated by ABAQUS and our IGA program for three cases, respectively. These three cases are described as follows:

1. Case 1: As shown in Fig. 8a, the left boundary is clamped and the right boundary is subjected to a prescribed traction force with $\boldsymbol{\sigma}_1 = 200N/mm^2$. Plane stress element is assumed to simulate the secondary creep. Figures 8b and 8c present the displacement contours obtained by using IGA and ABAQUS.
2. Case 2: As given in Fig. 9a, the bottom and left boundaries are clamped. The right and the top boundaries are subjected to a prescribed traction force with $\boldsymbol{\sigma}_1 = 200N/mm^2$. Plane stress element is used to simulate the primary creep. The displacement contours are provided in Figs. 9b and 9c.
3. Case 3: As given in Fig. 10a, the bottom and left boundaries are clamped. The right and the top boundaries are subjected to a prescribed traction force with $\boldsymbol{\sigma}_1 = 200N/mm^2$ and $\boldsymbol{\sigma}_2 = 100N/mm^2$. Plane strain element is used to simulate the secondary creep. The displacement results are given in Figs. 10b and 10c.

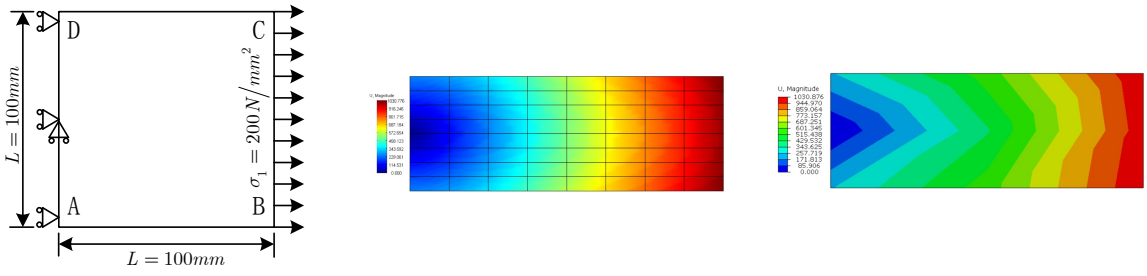

(a) Problem description (b) IGA result (c) ABAQUS result

Figure 8: Problem description and displacement (units: mm) result in comparison in Case 1. (a) the description and boundary condition of the square plate, (b) the result from IGA program, (c) the result from ABAQUS.

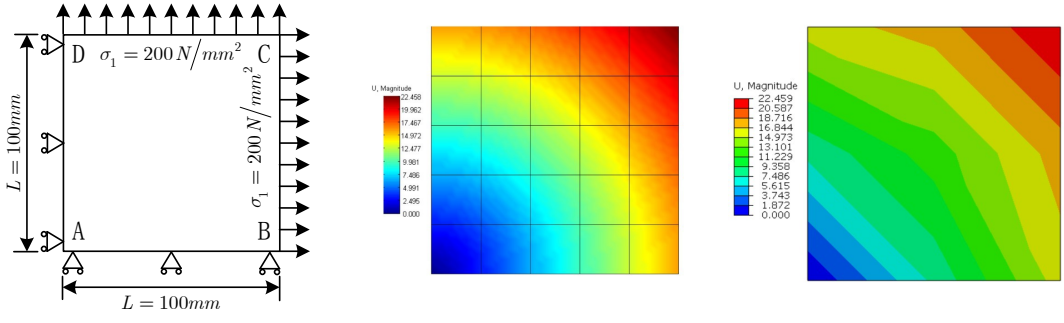

(a) Problem description (b) IGA result (c) ABAQUS result

Figure 9: Problem description and displacement (units: mm) result in comparison in Case 2. (a) the description and boundary condition of the square plate, (b) the result from IGA program, (c) the result from ABAQUS.

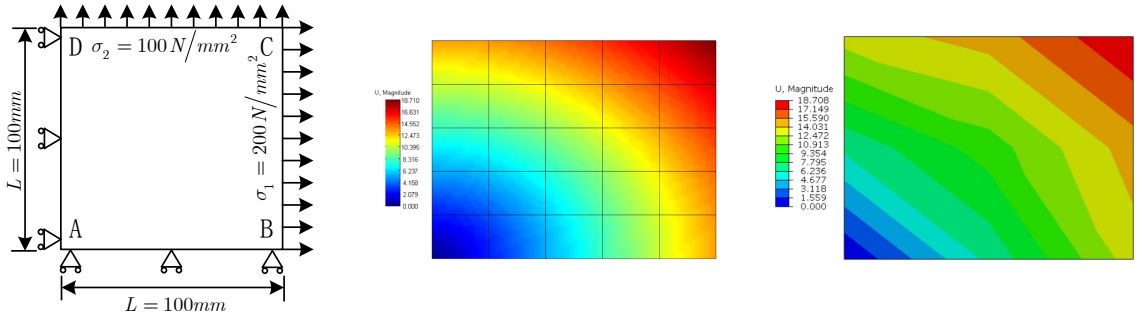

(a) Problem description (b) IGA result (c) ABAQUS result

Figure 10: Problem description and displacement (units: mm) result in comparison in Case 3. (a) the description and boundary condition of the square plate, (b) the result from IGA program, (c) the result from ABAQUS.

Material properties including Young's modulus $E = 2.0 \times 10^5 N/mm^2$, Poisson ratio $\nu = 0.3$ and $m = -0.5$ are used. The total creep time for these tests is set as 1000 hours.

From the comparison of the displacement contours given in Figs. 8, 9 and 10, it can be found that the IGA results agree very well with that of ABAQUS. As shown in Fig. 11, the relationships between time and the magnitude of displacement for the above creep examples are compared between using IGA and FEA in ABAQUS,respectively. It can be found that for each example, the displacement-time curves obtained by using different methods agree well with each other. Note that the curve in Fig. 11b agrees with the Eq. (22) which expresses the non-linear relationship between the creep strain rate and time. While the curves in Figs. 11a and 11c reflect the linearity of the Eq. (21).

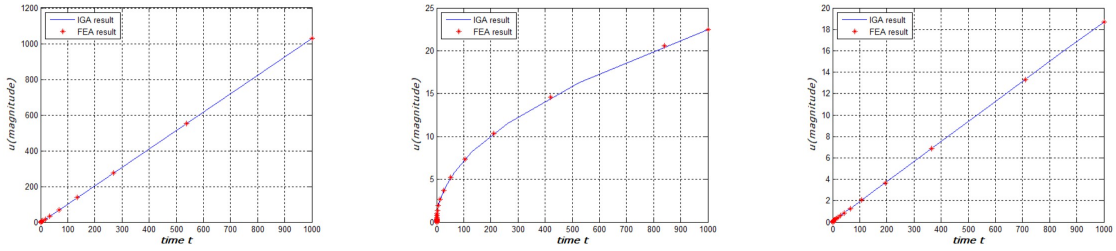

(a) Creep problem in Fig. 8 (b) Creep problem in Fig. 9 (c) Creep problem in Fig. 10

Figure 11: The displacement-time curve for the three creep cases obtained by IGA and FEA in ABAQUS. The horizontal axis denotes time (units: sec) and the vertical axis denotes the magnitude of displacement (units: mm) on the top right corner of the square plate.

6 CONCLUSIONS

In practical engineering, some mechanical parts are always working under high temperatures, e.g., aeroengine gas turbines. The simulation of such cases should consider the viscoplasticity of the materials and the high temperature creep problem, which may result in severe consequences if such deformations are ignorant by the service maintainers. To cope with this, the monitoring strategy needs a highly flexible pattern and in the real operation, fast measurement as well as rapid analysis are of priority. The isogeometric analysis will be an ideal tool for such scenarios, for its advantages of single model representation and more simplifying overall process. More specifically, finite element analysis needs to discrete CAD spline models into mesh models to carry out the simulation, which is time-consuming and introduces operations of model fixing, thus influences the analysis efficiency. In addition, since no lengthy mesh generation procedure is needed, the rapid response of isogeometric analysis plays a potentially important role in the development of digital twin concept and the simulation is pivotal for the fulfillment of effective digital twin deployment especially in the service stage of some complex products. So it's of long-term benefits to assess the capability of IGA for viscoplasticity and creep phenomena. In this paper, isogeometric analysis has been detailedly formulated and successfully employed for the simulation of viscoplasticity and creep problems. Several classical benchmark examples are investigated by using IGA and FEA to verify the proposed approach. Start from the numerical results already obtained, which prove the IGA as effective as FEA, future works will focus on the isogeometric analysis of more practical problems based on complexgeometric models and near real working conditions.

ACKNOWLEDGEMENTS

This research is supported by the Natural Science Foundation of China (Project Nos. 61572056 and 61972011).

ORCID

Ran Zhang http://orcid.org/0000-0002-9575-9006
Xiaoxiao Du http://orcid.org/0000-0002-2324-1005

REFERENCES

[1] Abaqus: Abaqus user's manual. version 6.14, 2014.

[2] Alfano, G.; De Angelis, F.; Rosati, L.: General solution procedures in elasto/viscoplasticity. Computer Methods in Applied Mechanics and Engineering, 190(39), 5123–5147, 2001. http://doi.org/10.1016/S0045-7825(00)00370-4.

[3] Ambati, M.; Kiendl, J.; De Lorenzis, L.: Isogeometric kirchhoff-love shell formulation for elasto-plasticity. Computer Methods in Applied Mechanics & Engineering, 340(OCT.1), 320–339, 2018. http://doi.org/10.1016/j.cma.2018.05.023.

[4] Armero, F.: Elastoplastic and Viscoplastic Deformations in Solids and Structures, 2017. http://doi.org/10.1002/9781119176817.ecm2029.

[5] Bazilevs, Y.; Calo, V.M.; Hughes, T.J.R.; Zhang, Y.: Isogeometric fluid-structure interaction: theory, algorithms, and computations. Computational Mechanics, 43(1), 3–37, 2008. http://doi.org/10.1007/s00466-008-0315-x.

[6] Bazilevs, Y.; Calo, V.M.; Zhang, Y.; Hughes, T.J.R.: Isogeometric fluid-structure interaction analysis with applications to arterial blood flow. Computational Mechanics, 38, 310–322, 2006. http://doi.org/10.1007/s00466-006-0084-3.

[7] Benson, D.J.; Bazilevs, Y.; Hsu, M.; Hughes, T.J.R.: A large deformation, rotation-free, isogeometric shell. Computer Methods in Applied Mechanics and Engineering, 200(13), 1367–1378, 2011. http://doi.org/10.1016/j.cma.2010.12.003.

[8] Benson, D.J.; Bazilevs, Y.; Hsu, M.C.; Hughes, T.J.R.: Isogeometric shell analysis: The reissner-mindlin shell. Computer Methods in Applied Mechanics & Engineering, 199(5-8), 276–289, 2010. http://doi.org/10.1016/j.cma.2009.05.011.

[9] Betten, J.: Creep mechanics (Third Edition), 2008. http://doi.org/10.1007/978-3-540-85051-9.

[10] Bower, A.: Applied Mechanics of Solids, 2009. http://doi.org/10.1136/bmj.1.4138.710-b.

[11] Cottrell, J.A.; Hughes, T.J.; Bazilevs, Y.: Isogeometric analysis: toward integration of CAD and FEA. John Wiley & Sons, 2009.

[12] da C. Andrade; N., E.: On the viscous flow in metals, and allied phenomena. Proceedings of the Royal Society of London, 84(567), 1–12, 1910. http://doi.org/10.1098/rspa.1910.0050.

[13] De Lorenzis, L.; Temizer, I.; Wriggers, P.; Zavarise, G.: A large deformation frictional contact formulation using nurbs-based isogeometric analysis. International Journal for Numerical Methods in Engineering, 87(13), 1278–1300, 2011. http://doi.org/10.1002/nme.3159.

[14] Du, X.; Zhao, G.; Wang, W.: Nitsche method for isogeometric analysis of reissner-mindlin plate with non-conforming multi-patches. Computer Aided Geometric Design, 35, 121–136, 2015. http://doi.org/10.1016/j.cagd.2015.03.005.

[15] Du, X.; Zhao, G.; Wang, W.; Fang, H.: Nitsche's method for non-conforming multipatch coupling in hyperelastic isogeometric analysis. Computational Mechanics, 65, 687–710, 2020. http://doi.org/10.1007/s00466-019-01789-x.

[16] Du, X.; Zhao, G.; Wang, W.; Mayi, G.; Zhang, R.; Yang, J.: Nliga: A matlab framework for nonlinear isogeometric analysis. Computer Aided Geometric Design, 101869, 2020. http://doi.org/10.1016/j.cagd.2020.101869.

[17] Freed, A.D.; Walker, K.P.: Viscoplasticity with creep and plasticity bounds. International Journal of Plasticity, 9(2), 213–242, 1993. http://doi.org/10.1016/0749-6419(93)90030-T.

[18] García Garino, C.; Ribero Vairo, M.S.; Andía Fagés, S.; Mirasso, A.E.; Ponthot, J.P.: Numerical simulation of finite strain viscoplastic problems. Journal of Computational & Applied Mathematics, 246, 174–184, 2013. http://doi.org/10.1016/j.cam.2012.10.008.

[19] Garino, C.G.; Vairo, M.S.R.; Fages, S.A.; Mirasso, A.; Ponthot, J.: Numerical simulation of finite strain viscoplastic problems. Journal of Computational and Applied Mathematics, 246(1), 174–184, 2013. http://doi.org/10.1016/j.cam.2012.10.008.

[20] Ghosh, S.; Kikuchi, N.: An arbitrary lagrangian-eulerian finite element method for large deformation analysis of elastic-viscoplastic solids. Computer Methods in Applied Mechanics & Engineering, 86(2), 127–188, 1991. http://doi.org/10.1016/0045-7825(91)90126-q.

[21] González, J.M.; Canet, J.M.; Oller, S.; Miró, R.: A viscoplastic constitutive model with strain rate variables for asphalt mixtures-numerical simulation. Computational Materials Science, 38(4), 0–560, 2007. http://doi.org/10.1016/j.commatsci.2006.03.013.

[22] Greenwood, G.W.: Comparisons of elastic and creep deformation linearly dependent upon stress. Materials Science and Technology, 25(4), 533–541, 2009. http://doi.org/10.1179/174328408x322105.

[23] Hughes, T.J.; Cottrell, J.A.; Bazilevs, Y.: Isogeometric analysis: CAD, finite elements, NURBS, exact geometry and mesh refinement. Computer methods in applied mechanics and engineering, 194(39), 4135–4195, 2005. http://doi.org/10.1016/j.cma.2004.10.008.

[24] Hughes, T.J.; Taylor, R.L.: Unconditionally stable algorithms for quasi-static elasto/visco-plastic finite element analysis. Computers & Structures, 8(2), 169–173, 1978. http://doi.org/10.1016/0045-7949(78)90019-6.

[25] Kiendl, J.; Hsu, M.; Wu, M.C.H.; Reali, A.: Isogeometric kirchhoff-love shell formulations for general hyperelastic materials. Computer Methods in Applied Mechanics and Engineering, 291, 280–303, 2015. http://doi.org/10.1016/j.cma.2015.03.010.

[26] Kim, N.H.: Introduction to Nonlinear Finite Element Analysis, 2015. http://doi.org/10.1007/978-1-4419-1746-1.

[27] Lee, S.J.; Kim, H.R.: Vibration and buckling of thick plates using isogeometric approach. Architectural research, 15(1), 35–42, 2013. http://doi.org/10.5659/AIKAR.2013.15.1.35.

[28] Leon, E.P.; Aliabadi, M.H.; Ortizdominguez, M.: Boundary element analysis for primary and secondary creep problems. Revista Mexicana De Fisica, 54(5), 341–348, 2008.

[29] Lubliner, J.: On the structure of the rate equations of materials with internal variables. Acta Mechanica, 17(1-2), 109–119, 1973. http://doi.org/10.1007/bf01260883.

[30] Mitsoulis, E.: Flows of Viscoplastic Materials: Models and Computations, 2007.

[31] Naumenko, K.; Altenbach, H.: Modeling of Creep for Structural Analysis. Springer Berlin Heidelberg, 2007. http://doi.org/10.1007/978-3-540-70839-1_1.

[32] Neto; EduardodeSouza: Computational methods for plasticity:theory and applications, 2008. http://doi.org/10.1002/9780470694626.fmatter.

[33] Nguyen, D.K.; Nguyen-Xuan, H.: Isogeometric analysis of linear isotropic and kinematic hardening elasto-plasticity. Vietnam Journal of Mechanics, 38, 2016. http://doi.org/10.15625/0866-7136/7817.

[34] Owen, D.R.J.; Hinton, E.: Finite elements in plasticity: theory and practice, 1980.

[35] Perzyna; P.: The constitutive equations for rate sensitive plastic materials. Quart.appl.math, 20(4), 321–332, 1963. http://doi.org/10.1090/qam/144536.

[36] Perzyna, P.: Fundamental problems in viscoplasticity. Adv.appl.mech, 9(2), 243–377, 1966. http://doi.org/10.1016/S0065-2156(08)70009-7.

[37] Piegl, L.A.; Tiller, W.: The NURBS book., 1997. http://doi.org/10.1007/978-3-642-59223-2.

[38] Reddy, J.N.: Theory and Analysis of Elastic Plates and Shells, vol. 99, 1999. http://doi.org/10.1021/ja00444a065.

[39] Rice; J., R.: On the structure of stress-strain relations for time-dependent plastic deformation in metals. Journal of Applied Mechanics, 37(3), 1969. http://doi.org/10.1115/1.3408603.

[40] Seo, Y.; Kim, H.; Youn, S.: Isogeometric topology optimization using trimmed spline surfaces. Computer Methods in Applied Mechanics and Engineering, 199(49), 3270–3296, 2010. http://doi.org/10.1016/j.cma.2010.06.033.

[41] Shojaee, S.; Izadpanah, E.; Valizadeh, N.; Kiendl, J.: Free vibration analysis of thin plates by using a nurbs-based isogeometric approach. Finite Elements in Analysis and Design, 61, 23–34, 2012. http://doi.org/10.1016/j.finel.2012.06.005.

[42] Simo, J.; Hughes: Computational Inelasticity, 2000. http://doi.org/10.1007/b98904.

[43] Simo, J.C.; Kennedy, J.G.; Govindjee, S.: Non-smooth multisurface plasticity and viscoplasticity. loading/unloading conditions and numerical algorithms. International Journal for Numerical Methods in Engineering, 26(10), 2161–2185, 1988. http://doi.org/10.1002/nme.1620261003.

[44] Veiga, L.B.D.; Buffa, A.; Lovadina, C.; Martinelli, M.; Sangalli, G.: An isogeometric method for the reissner-mindlin plate bending problem. Computer Methods in Applied Mechanics and Engineering, 209, 45–53, 2012. http://doi.org/10.1016/j.cma.2011.10.009.

[45] Wall, W.A.; Frenzel, M.A.; Cyron, C.: Isogeometric structural shape optimization. Computer Methods in Applied Mechanics & Engineering, 197(33-40), 2976–2988, 2008. http://doi.org/10.1016/j.cma.2008.01.025.

[46] Winnicki, A.; Pearce, C.J.; Bieanie, N.: Viscoplastic hoffman consistency model for concrete. Computers & Structures, 79(1), p.7–19, 2001. http://doi.org/10.1016/s0045-7949(00)00110-3.

[47] Zhao, G.; Du, X.; Wang, W.; Liu, B.; Fang, H.: Application of isogeometric method to free vibration of reissner-mindlin plates with non-conforming multi-patch. Computer-Aided Design, 82, 127–139, 2017. http://doi.org/10.1016/j.cad.2016.04.006.

[48] Zienkiewicz, O.C.; Cormeau, I.C.: Visco-plasticity-plasticity and creep in elastic solids-a unified numerical solution approach. International Journal for Numerical Methods in Engineering, 8(4), 821–845, 1974. http://doi.org/10.1002/nme.1620080411.

[49] Zienkiewicz, O.C.; Taylor, R.L.: The Finite Element Method, 2005. http://doi.org/10.1007/0-387-26160-5_6.